sciendo RIGA TECHNICAL UNIVERSITY 1862
Electrical, Control and Communication Engineering
ISSN 2255-9159 (online)
ISSN 2255-9140 (print)
2018, vol. 14, no. 2, pp. 134–140
doi: 10.2478/ecce-2018-0016
https://content.sciendo.com

Phase Characteristics of Models of GaAs Gyroelectric Waveguides with Temperature Sensitive Anisotropic Dielectric Layers in Case of One Layer

Darius Plonis* (*Associate Professor, Vilnius Gediminas Technical University, Vilnius, Lithuania*),
Andrius Katkevičius (*Associate Professor, Vilnius Gediminas Technical University, Vilnius, Lithuania*),
Diana Belova-Plonienė (*Specialist, Vilnius Gediminas Technical University, Vilnius, Lithuania*)

Abstract **– Models of open cylindrical multilayer gyroelectric-anisotropic-gyroelectric waveguides are presented in this paper. The influence of density of free carriers, temperature and the presence of the external dielectric layer on the wave phase characteristics of the models of *n*-GaAs waveguides has been evaluated. Differential Maxwell's equations, coupled mode and partial area methods have been used to obtain complex dispersion equation of the models of gyroelectric-anisotropic-gyroelectric waveguides with or without the temperature sensitive external anisotropic dielectric layer. The analysis has shown that the phase characteristics are practically unchanged when the density of electrons is equal to $N = (10^{17}–5\cdot10^{18})$ m^{-3}, $d/r^s = 0$, the changes of wave phase coefficients are obtained in the models of waveguides with the external anisotropic dielectric layer. The largest differences of wave phase coefficient are obtained when the density of electrons is $N = 10^{21}$ m^{-3}. The external dielectric layer improves the control of gyroelectric *n*-GaAs waveguides with temperature.**

Keywords **– Microwave propagation; Propagation constant; Semiconductor waveguides.**

I. Introduction

Waveguides are used in many types of microwave devices: phase shifters [1], telecommunications [2] and many other [3]. Quickly evolving technologies require the development of new structures of waveguides and research into new materials, which could be used in the production of waveguides.

For example, [4], [5] use graphene-based waveguides to address polarization issues. The model of a planar dielectric waveguide with two-dimensional semiconductors is presented in [6]. The authors have provided computational illustrations of potentially strong effects and considered interesting opportunities that may result from integration of 2D semiconductors into dielectric waveguides.

The authors of [7], [8] have used the plasmonic material in the investigation of waveguides. Results of [7] have demonstrated that the hybrid plasmonics slot THz waveguide provides significantly enhanced field confinement in low index slot regions: more than five times that of traditional low index slot waveguides.

Modes of dielectric or ferrite gyrotropic slab and circular waveguides are investigated using analytical methods based on Maxwell's equations in [9]. The authors have used the gyrotropic material of dielectric or ferrite type, where either the permittivity or the permeability tensor is altered by a longitudinally applied quasistatic magnetic field. The solution of fast phase shifter using ferrite waveguide is presented in [10]. The authors have designed waveguide for the ferrite phase shifters of reduced diameter. The reduction of cross-sectional size of the ferrite phase shifter was achieved by selection of ferrite materials with $\mu_2(B_r)$ equal to 0.28 and 0.42 for ferrite rod and magnetic cores, respectively. The authors of [11] have used the dielectric waveguide for the development of continuously tunable w-band phase shifter.

External layers or shields are another important element of waveguides. Semi-shielded dielectric waveguides are investigated in [12]. The cylindrical waveguide with an external layer of metamaterial is presented and investigated in [13]. The authors claim that the surface modes of a metamaterial dielectric waveguide with comparable electric and magnetic losses can be less lossy than the surface modes of an analogous metal-dielectric waveguide with electric losses alone. Metamaterial waveguide devices for integrated optics are presented in [14]. The usage of different materials in waveguides is widely described in many articles [15], [16].

The aim of this paper is to investigate wave phase characteristics in models of gyroelectric-anisotropic-gyroelectric *n*-GaAs waveguides with or without a temperature sensitive external anisotropic dielectric layer. It is also intended to investigate how phase characteristics depend on the density of free carriers and temperature in gyroelectric *n*-GaAs waveguides, when only one temperature sensitive external anisotropic dielectric layer is used.

II. Methods and Materials

A. Methods

The electrodynamical model of open cylindrical multilayer gyroelectric-anisotropic-gyroelectric waveguides is shown in Fig. 1. The model consists of several parts: Area 1 is the gyroelectric material; Areas 2_1 and 2_2 are the external anisotropic dielectric layers; Area 3 is a gyroelectric or air material. The parameters of these areas are presented in the caption of Fig. 1.

The Maxwell's complex differential equations, coupled mode and boundary conditions methods are used in order to

* Corresponding author.
E-mail: darius.plonis@vgtu.lt

obtain the complex dispersion equation of models of multilayer gyroelectric-anisotropic/isotropic-gyroelectric waveguides. The longitudinal components of electric and magnetic fields in gyrotropic core are $\underline{E}_z^{\mathrm{g1}}$ and $\underline{H}_z^{\mathrm{g1}}$ respectively. The equations of longitudinal components of electric and magnetic fields in gyrotropic core are presented in [17].

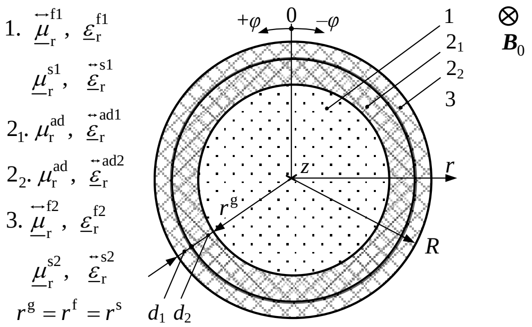

Fig. 1. The electrodynamical model of the open cylindrical multilayer gyroelectric-anisotropic-gyroelectric waveguide, where: $\underline{\underline{\varepsilon}}_{\mathrm{r}}^{\mathrm{g1}}$ is the complex permittivity tensor of gyroelectric core; $\underline{\mu}_{\mathrm{r}}^{\mathrm{g1}}$ is the complex permeability of gyroelectric core; $\mu_{\mathrm{r}}^{\mathrm{ad1}}$ is the permeability of the first anisotropic dielectric layer; $\underline{\underline{\varepsilon}}_{\mathrm{r}}^{\mathrm{ad1}}$ is the complex permittivity tensor of the first anisotropic dielectric layer; $\mu_{\mathrm{r}}^{\mathrm{ad2}}$ is the permeability of the second anisotropic dielectric layer; $\underline{\underline{\varepsilon}}_{\mathrm{r}}^{\mathrm{ad2}}$ is the complex permittivity tensor of the second anisotropic dielectric layer; $\underline{\underline{\varepsilon}}_{\mathrm{r}}^{\mathrm{g2}}$ is the complex permittivity tensor of gyroelectric material; $\underline{\mu}_{\mathrm{r}}^{\mathrm{g2}}$ is the complex permeability of gyroelectric material; B_0 is a vector of magnetic flux density; R_1 and R_2 are the radii of the anisotropic dielectric layers, d_1 and d_2 are widths of the anisotropic dielectric layers and r^{g} is the radius of the gyroelectric core.

The longitudinal components of electric and magnetic fields, which satisfy Maxwell's equations in anisotropic dielectric layers (Areas 2_1 and 2_2) of the model (Fig. 1), can be presented as:

$$\underline{E}_z^{\mathrm{ad},(i)} = \left[\underline{A}_{1+i}\,\mathrm{J}_m(\underline{k}_{\perp1}^{\mathrm{ad},i} r^{\mathrm{g}}) + \underline{A}_{2+i}\,\mathrm{Y}_m(\underline{k}_{\perp1}^{\mathrm{ad},i} r^{\mathrm{g}}) \right] \mathrm{e}^{\mathrm{j}\varphi}; \quad (1)$$

$$\underline{H}_z^{\mathrm{ad},(i)} = \left[\underline{B}_{1+i}\,\mathrm{J}_m(\underline{k}_{\perp2}^{\mathrm{ad},i} r^{\mathrm{g}}) + \underline{B}_{2+i}\,\mathrm{Y}_m(\underline{k}_{\perp2}^{\mathrm{ad},i} r^{\mathrm{g}}) \right] \mathrm{e}^{\mathrm{j}\varphi}, \quad (2)$$

where $\underline{A}_{1+i}$; $\underline{A}_{2+i}$ and $\underline{B}_{1+i}$; $\underline{B}_{2+i}$ are unknown amplitude coefficients for different external dielectric layers; $\mathrm{J}_m(\underline{k}_{\perp1,2}^{\mathrm{ad},i} r^{\mathrm{g}})$ is the Bessel function of the first kind of the m-th order with the complex arguments $\underline{k}_{\perp1,2}^{\mathrm{ad},i} r^{\mathrm{g}}$; $\mathrm{Y}_m(\underline{k}_{\perp1,2}^{\mathrm{ad},i} r^{\mathrm{g}})$ is the Bessel (Neumann) function of the second kind of the m-th order with the complex arguments; $\underline{k}_{\perp1,2}^{\mathrm{ad},i}$ are numbers of the transversal waves in anisotropic dielectric layers; m is the first (azimuthal) index of the hybrid mode, which describes the constant component of the longitudinal wave by the azimuthal perimeter coordinate φ; $\mathrm{j} = \sqrt{-1}$ is the complex number; i is the number of external anisotropic dielectric layers (i = 1; 2 (these numbers mean lower index of second area of the model)).

Numbers of transversal waves in the anisotropic (isotropic) dielectric layers can be presented as:

$$\underline{k}_{\perp1}^{\mathrm{ad},i} = \sqrt{k^2 \underline{\varepsilon}_{xx}^{\mathrm{ad},i} - \underline{\gamma}^2}; \quad (3)$$

$$\underline{k}_{\perp2}^{\mathrm{ad},i} = \sqrt{\frac{\underline{\varepsilon}_{zz}^{\mathrm{ad},i}}{\underline{\varepsilon}_{xx}^{\mathrm{ad},i}} \left(k^2 \underline{\varepsilon}_{xx}^{\mathrm{ad},i} - \underline{\gamma}^2 \right)}, \quad (4)$$

where $\underline{\gamma} = h' - \mathrm{j}h''$ is the complex propagation constant (here $h' = \mathrm{Re}(\underline{\gamma}) = 2\pi / \lambda_{\mathrm{w}}$ is the phase coefficient and λ_{w} is the wavelength of the waveguide modes; $h'' = \mathrm{Im}(\underline{\gamma})$ is the attenuation coefficient); $k = \omega/c$ is the wave number in a vacuum; $\underline{\varepsilon}_{xx}^{\mathrm{ad},i}$ and $\underline{\varepsilon}_{zz}^{\mathrm{ad},i}$ are diagonal elements of tensors of the anisotropic dielectric layers for the different external dielectric layers.

Area 3 of the model (Fig. 1) could be isotropic (for example, it could be air), anisotropic or gyroelectric material. The longitudinal components of electric and magnetic fields in the isotropic material are:

$$\underline{E}_z^{\mathrm{is}} = \underline{A}_7 \mathrm{H}_m^{(2)}(\underline{k}_{\perp}^{\mathrm{is}} r^{\mathrm{g}}) \mathrm{e}^{\mathrm{j}\varphi}; \quad (5)$$

$$\underline{H}_z^{\mathrm{is}} = \underline{A}_8 \mathrm{H}_m^{(2)}(\underline{k}_{\perp}^{\mathrm{is}} r^{\mathrm{g}}) \mathrm{e}^{\mathrm{j}\varphi}, \quad (6)$$

where $\underline{A}_7$ and $\underline{A}_8$ are unknown amplitude coefficients; $\mathrm{H}_m^{(2)}(\underline{k}_{\perp}^{\mathrm{is}} r^{\mathrm{g}})$ is the Bessel (Hankel function of the second kind) function of the third kind of the m-th order with the complex argument; $\underline{k}_{\perp}^{\mathrm{is}} r^{\mathrm{g}}$ is the number of transversal waves in the isotropic material. The number of transversal waves in the isotropic material can be presented as:

$$\underline{k}_{\perp}^{\mathrm{is}} = \sqrt{k^2 \underline{\varepsilon}_{\mathrm{r}}^{\mathrm{is}} \underline{\mu}_{\mathrm{r}}^{\mathrm{is}} - \underline{\gamma}}\,, \quad (7)$$

where $\underline{\varepsilon}_{\mathrm{r}}^{\mathrm{is}}$, $\underline{\mu}_{\mathrm{r}}^{\mathrm{is}}$ are the complex permittivity and permeability of the isotropic material. $\underline{\varepsilon}_{\mathrm{r}}^{\mathrm{is}} = \underline{\mu}_{\mathrm{r}}^{\mathrm{is}} = 1$ means that Area 3 of the model is air. $\underline{\varepsilon}_{\mathrm{r}}^{\mathrm{is}} > 1$, $\underline{\mu}_{\mathrm{r}}^{\mathrm{is}} > 1$ means that Area 3 of the model is an isotropic material.

The longitudinal components of electric and magnetic fields in the anisotropic material are:

$$\underline{E}_z^{\mathrm{an}} = \underline{A}_7 \mathrm{H}_m^{(2)}(\underline{k}_{\perp1}^{\mathrm{an}} r^{\mathrm{g}}) \mathrm{e}^{\mathrm{j}\varphi}; \quad (8)$$

$$\underline{H}_z^{\mathrm{an}} = \underline{B}_7 \mathrm{H}_m^{(2)}(\underline{k}_{\perp2}^{\mathrm{an}} r^{\mathrm{g}}) \mathrm{e}^{\mathrm{j}\varphi}, \quad (9)$$

where $\underline{B}_7$ is the unknown amplitude coefficient; $\underline{k}_{\perp1,2}^{\mathrm{an}}$ are numbers of the transversal waves in anisotropic material. Numbers of the transversal waves in the anisotropic material are similar to equations (3) and (4). The main difference is only in $\underline{\varepsilon}_{xx}^{\mathrm{an}}$ and $\underline{\varepsilon}_{zz}^{\mathrm{an}}$ expressions. Area 3 is the isotropic material and numbers of transversal waves are equal ($\underline{k}_{\perp1}^{\mathrm{an}} = \underline{k}_{\perp2}^{\mathrm{an}} = \underline{k}_{\perp}^{\mathrm{is}}$) in the anisotropic and isotropic material if the diagonal elements of the complex tensor of anisotropic material are equal ($\underline{\varepsilon}_{xx}^{\mathrm{an}} = \underline{\varepsilon}_{zz}^{\mathrm{an}} = \underline{\varepsilon}_{\mathrm{r}}^{\mathrm{is}}$).

The longitudinal components of electric and magnetic fields in the gyroelectric material (Area 3) are:

$$\underline{E}_z^{\mathrm{g2}} = \left[\underline{a}^{\mathrm{g2}} \underline{A}_7 \mathrm{H}_m (\underline{k}_{\perp 1}^{\mathrm{g2}} r^{\mathrm{g}}) + \underline{B}_7 \mathrm{H}_m (\underline{k}_{\perp 2}^{\mathrm{g2}} r^{\mathrm{g}}) \right] \mathrm{e}^{\mathrm{j}\varphi}; \quad (10)$$

$$\underline{H}_z^{\mathrm{g2}} = \left[\underline{A}_7 \mathrm{H}_m (\underline{k}_{\perp 1}^{\mathrm{g2}} r^{\mathrm{g}}) + \underline{b}^{\mathrm{g2}} \underline{B}_7 \mathrm{H}_m (\underline{k}_{\perp 2}^{\mathrm{g2}} r^{\mathrm{g}}) \right] \mathrm{e}^{\mathrm{j}\varphi}; \quad (11)$$

where $\underline{k}_{\perp 1,2}^{\mathrm{g2}}$ are numbers of the transversal waves of the second gyroelectric material; $\underline{a}^{\mathrm{g2}}$ and $\underline{b}^{\mathrm{g2}}$ are H- and E- waves mixing ratio of the hybrid waves. Expressions of $\underline{a}^{\mathrm{g2}}$; $\underline{b}^{\mathrm{g2}}$; $\underline{k}_{\perp 1}^{\mathrm{g2}}$; $\underline{k}_{\perp 2}^{\mathrm{g2}}$ are presented in [17]. The gyroelectric material transforms into the isotropic material if the magnetic flux density is equal to 0 ($B_0 = 0$ T) because elements of the complex tensors are equal $\underline{\varepsilon}_{xx}^{\mathrm{g2}} = \underline{\varepsilon}_{zz}^{\mathrm{g2}} = \underline{\varepsilon}_{\mathrm{r}}^{\mathrm{is}}$ and $\underline{\varepsilon}_{xy}^{\mathrm{g2}} = 0$. Area 3 of the model could be the anisotropic material as well, when $\underline{\varepsilon}_{xx}^{\mathrm{g2}} = \underline{\varepsilon}_{xx}^{\mathrm{an}}$, $\underline{\varepsilon}_{zz}^{\mathrm{g2}} = \underline{\varepsilon}_{zz}^{\mathrm{an}}$ and $\underline{\varepsilon}_{xy}^{\mathrm{g2}} = 0$. In this case, numbers of the transversal waves in the second gyroelectric material will be the same as in the anisotropic material $\underline{k}_{\perp 1}^{\mathrm{g2}} = \underline{k}_{\perp 1}^{\mathrm{an}}$ and $\underline{k}_{\perp 2}^{\mathrm{g2}} = \underline{k}_{\perp 2}^{\mathrm{an}}$, in other words, the main equations of the longitudinal components of electric and magnetic fields in Area 3 are (10) and (11).

The azimuthal components of electric $\underline{E}_{\varphi}^{\mathrm{g1,ad},(i),\mathrm{is,an,g2}}$ and magnetic $\underline{H}_{\varphi}^{\mathrm{g1,ad},(i),\mathrm{is,an,g2}}$ fields in different materials (areas of the model Figure 1) could be obtained from longitudinal components $\underline{E}_z^{\mathrm{g1,ad},(i),\mathrm{is,an,g2}}$ and $\underline{H}_z^{\mathrm{g1,ad},(i),\mathrm{is,an,g2}}$. Certain part of these azimuthal comments was presented in [17].

The complex dispersion equation is obtained by using boundary conditions. The complex dispersion equation of the model of multilayer gyroelectric-anisotropic-gyroelectric waveguides (Fig. 1) is the 12-th order determinant (see Fig. 2) expression $\underline{D} = \det[\underline{a}_{jk}] = 0$, where j is a column and k is a row index of determinant and $\underline{a}_{jk}$ are complex elements of determinant.

The determinant consists of four parts: the part, which is noted by "g1", includes elements of determinant, which indicate the EM wave propagation in gyroelectric core; the part, which is noted by "ad1", includes elements of determinant, which indicate the EM wave propagation in the first anisotropic dielectric layer; the part, which is noted by "ad2", includes elements of determinant, which indicate the EM wave propagation in the second anisotropic dielectric layer, and the last part, which is noted by "g2", includes elements of determinant, which indicate the EM wave propagation in the gyroelectric material.

g1 g-ad1 ad1 ad1-ad2 ad2-g2

$$\begin{vmatrix}
\underline{a}_{11} & \underline{a}_{12} & \underline{a}_{13} & 0 & \underline{a}_{15} & 0 & 0 & 0 & 0 & 0 & 0 & 0 \\
\underline{a}_{21} & \underline{a}_{22} & 0 & \underline{a}_{24} & 0 & \underline{a}_{26} & 0 & 0 & 0 & 0 & 0 & 0 \\
\underline{a}_{31} & \underline{a}_{32} & \underline{a}_{33} & \underline{a}_{34} & \underline{a}_{35} & \underline{a}_{36} & 0 & 0 & 0 & 0 & 0 & 0 \\
\underline{a}_{41} & \underline{a}_{42} & \underline{a}_{43} & \underline{a}_{44} & \underline{a}_{45} & \underline{a}_{46} & 0 & 0 & 0 & 0 & 0 & 0 \\
0 & 0 & \underline{a}_{53} & 0 & \underline{a}_{55} & 0 & \underline{a}_{57} & 0 & \underline{a}_{59} & 0 & 0 & 0 \\
0 & 0 & 0 & \underline{a}_{64} & 0 & \underline{a}_{66} & 0 & \underline{a}_{68} & 0 & \underline{a}_{610} & 0 & 0 \\
0 & 0 & \underline{a}_{73} & \underline{a}_{74} & \underline{a}_{75} & \underline{a}_{76} & \underline{a}_{77} & \underline{a}_{78} & \underline{a}_{79} & \underline{a}_{710} & 0 & 0 \\
0 & 0 & \underline{a}_{83} & \underline{a}_{84} & \underline{a}_{85} & \underline{a}_{86} & \underline{a}_{87} & \underline{a}_{88} & \underline{a}_{89} & \underline{a}_{810} & 0 & 0 \\
0 & 0 & 0 & 0 & 0 & 0 & \underline{a}_{97} & 0 & \underline{a}_{99} & 0 & \underline{a}_{911} & \underline{a}_{912} \\
0 & 0 & 0 & 0 & 0 & 0 & 0 & \underline{a}_{108} & 0 & \underline{a}_{1010} & \underline{a}_{1011} & \underline{a}_{1012} \\
0 & 0 & 0 & 0 & 0 & 0 & \underline{a}_{117} & \underline{a}_{118} & \underline{a}_{119} & \underline{a}_{1110} & \underline{a}_{1111} & \underline{a}_{1112} \\
0 & 0 & 0 & 0 & 0 & 0 & \underline{a}_{127} & \underline{a}_{128} & \underline{a}_{129} & \underline{a}_{1210} & \underline{a}_{1211} & \underline{a}_{1212}
\end{vmatrix}$$

ad2 g2

Fig. 2. The complex dispersion equation of models of multilayer gyroelectric-anisotropic-gyroelectric waveguides.

The boundaries between the four areas are noted by "g1- ad1", "ad1-ad2" and "ad2-g2". "g1-ad1" is the boundary between the gyroelectric core and the first anisotropic dielectric layer. "ad1-ad2" is the boundary between the first anisotropic dielectric layer and the second anisotropic dielectric layer. "ad2-g2" is the boundary between the second anisotropic dielectric layer and the gyroelectric material.

The analysis of the presented model shows that the developed model is more universal than presented in other works [17], [18].

B. Materials

Only one temperature sensitive external anisotropic dielectric layer was selected in this investigation case. The thickness of the external anisotropic dielectric layer was equal to $d_1/r^s + d_2/r^s = d/r^s = 0.3$ (here $d_1/r^s = d_2/r^s = 0.15$), where r^s is the semiconductor (gyroelectric) core, $r^s = 1$ mm. The temperature sensitive external anisotropic dielectric layer consists of TM-15 and non-magnetic $Rb_{1-x}(ND_4)D_2PO_4$ ferroelectric dielectrics both of which are mixed by using (Maxwell's-Garnet's) material mixing expressions [19], [20]. The filling ratio of permittivities of dielectrics – N_d is 0.75 [19], [20].

The permittivity of TM-15 dielectric is $\varepsilon_r^{\mathrm{d}} = 15$. The permittivity of non-magnetic $Rb_{1-x}(ND_4)D_2PO_4$ ferroelectric depends on temperature, the dielectric properties of $Rb_{1-x}(ND_4)D_2PO_4$ were investigated in paper [21].

In this investigation case, Area 3 of the electrodynamical model of open cylindrical multilayer gyroelectric-anisotropic-gyroelectric waveguides (Fig. 1) is air and its permittivity and permeability are equal to 1.

III. Results

The models of n-GaAs gyroelectric waveguides were analyzed when the mobility of electrons varied depending on the temperature [22]:

$$\mu_n = 0.94(300\,/\,T)\ \mathrm{m^2\,V^{-1}\,s^{-1}}\,, \qquad (12)$$

where T is the absolute temperature of the semiconductors.

The dielectric constant of n-GaAs semiconductors was equal to $\varepsilon_r = 13.1$ and effective mass was equal to $m^* = 0.067m_e$, where m_e is the rest mass of electrons.

The phase characteristics are presented for the main type HE_{11} and the first higher type EH_{11} waves. Other higher type waves are parasitic and have not been explored. The phase characteristics of the models of the gyroelectric waveguides are presented as dependencies of the normalized phase coefficient – $h'r^s$ on the normalized frequency – fr^s.

These phase characteristics were received, when the polarization of the electromagnetic waves is left-hand $\exp(+jm\varphi)$, where m is the first azimuthal index of hybrid waves, $m = 1$.

The phase characteristics of the models of the gyroelectric, semiconductor and semiconductor-dielectric n-GaAs waveguides with different densities of electrons $N = 10^{17}$; $5{\cdot}10^{18}$; $5{\cdot}10^{19}$; 10^{20}; 10^{21} m^{-3} and temperatures T = 125; 150; 175; 200 K are presented in Figs 3–11.

Wave phase characteristics of n-GaAs semiconductor-dielectric devices when the density of electrons is equal to $N = 10^{17}$; $5{\cdot}10^{18}$ m^{-3} are presented in Figs 3 and 4. These characteristics are almost the same in both figures.

The phase characteristics are shifted to the lower frequencies when temperature T increases, but the variation of wave phase coefficient remains the same within the operating frequency range. Therefore, the usage of n-GaAs is not useful in phase shifters as it reduces the limits of the phase shifter.

The phase characteristics of the semiconductor and semiconductor-dielectric waveguides when the density of electrons is equal to $N = 5{\cdot}10^{19}$ m^{-3} are presented in Figs 6 and 7.

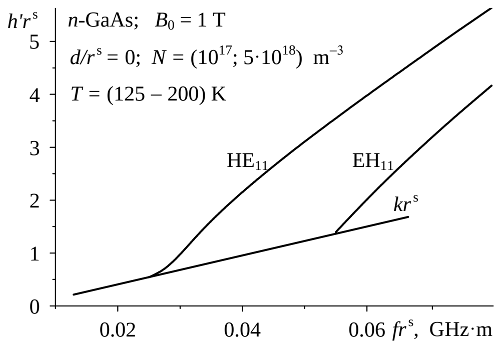

Fig. 3. Wave phase characteristics of models of gyroelectric n-GaAs semiconductor waveguides, when B_0 = 1 T; $N = (10^{17}–5{\cdot}10^{18})$ m^{-3}.

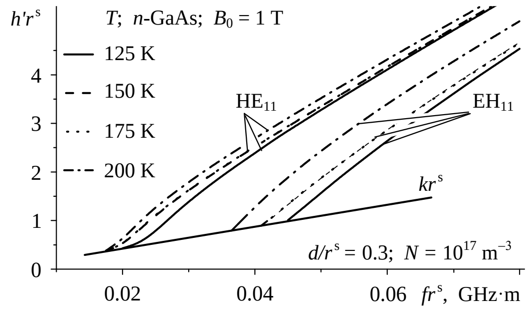

Fig. 4. Wave phase characteristics of models of gyroelectric n-GaAs semiconductor-dielectric waveguides, when $d/r^s = 0.3$; B_0 = 1 T; $N = 10^{17}$ m^{-3}.

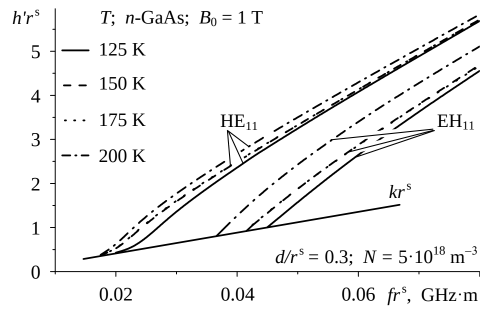

Fig. 5. Wave phase characteristics of models of gyroelectric n-GaAs semiconductor-dielectric waveguides, when $d/r^s = 0.3$; B_0 = 1 T; $N = 5{\cdot}10^{18}$ m^{-3}.

The insignificantly bigger phase shift to the lower frequencies side appears when temperature T is changing in the models of the waveguides without an external anisotropic dielectric $d/r^s = 0$ layer compared with the characteristics, which are given in Fig. 4.

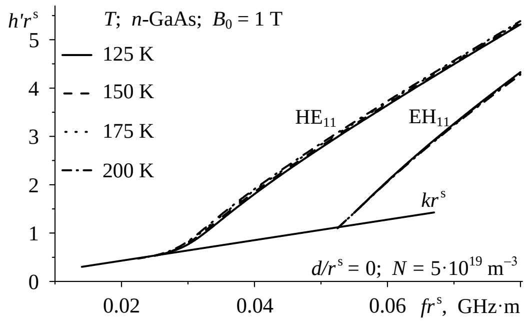

Fig. 6. Wave phase characteristics of models of gyroelectric n-GaAs semiconductor waveguides, when $d/r^s = 0$; B_0 = 1 T; $N = 5{\cdot}10^{19}$ m^{-3}.

The significantly larger change of the phase coefficient of the main type HE_{11} wave is obtained by using an external dielectric layer $Rb_{1-x}(ND_4)D_2PO_4$. The phase characteristics of the semiconductor-dielectric waveguides with the external dielectric layer are presented in Fig. 7. It could be seen that wave phase characteristics are shifted to the lower frequencies when the external anisotropic dielectric layer is used.

The bigger phase shift is obtained in the models of waveguides with the external anisotropic dielectric layer because the relative dielectric permittivity of one of the external dielectric layers depends on the temperature and frequency.

Waves phase characteristics when the density of electrons is equal to $N = 10^{20}$ m^{-3} are presented in Figs 8 and 9. The comparison of Figs 3, 6 and 8 shows that the biggest phase shift in waveguides without the external anisotropic dielectric layer $d/r^s = 0$ is obtained when the density of electrons is equal to $N = 10^{20}$ m^{-3} (Fig. 8).

It could be seen from Figs 8, 9 and Table I that the widest working frequency range in the models of the waveguides without the external dielectric layer is obtained when the temperature is equal to $T = 200$ K. The widest working frequency range in the models of the waveguides with the external anisotropic dielectric layer is obtained when the temperature is equal to $T = 175$ K. Working frequencies range of the models of the waveguides with the external anisotropic dielectric layer becomes wider as the temperature rises until 175 K. The widest working frequency range is equal to $\Delta fr^s = 0.0284$ GHz·m, at $T = 175$ K. The working frequency range begins to narrow at higher than 175 K temperatures. Such variation of working frequency range is related to the properties of n-GaAs semiconductor and $Rb_{1-x}(ND_4)D_2PO_4$ ferroelectric.

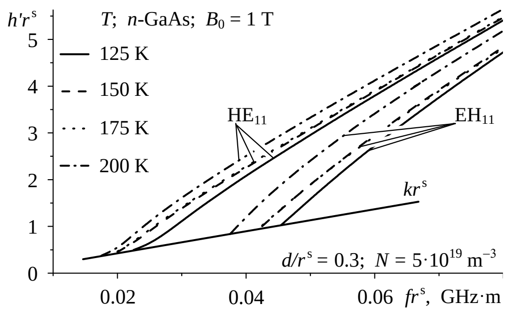

Fig. 7. Wave phase characteristics of models of gyroelectric n-GaAs semiconductor-dielectric waveguides, when $d/r^s = 0.3$; $B_0 = 1$ T; $N = 5 \cdot 10^{19}$ m^{-3}.

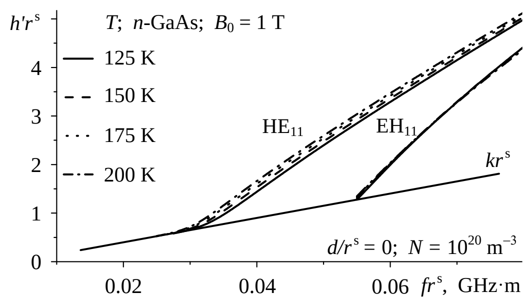

Fig. 8. Wave phase characteristics of models of gyroelectric n-GaAs semiconductor waveguides, when $d/r^s = 0$; $B_0 = 1$ T; $N = 10^{20}$ m^{-3}.

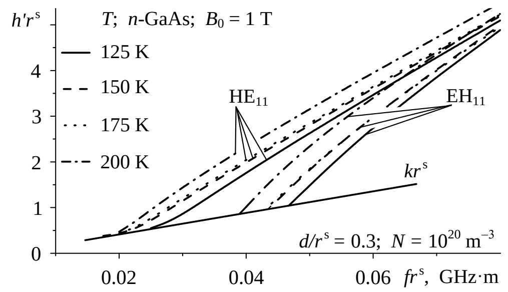

Fig. 9. Wave phase characteristics of models of gyroelectric n-GaAs semiconductor-dielectric waveguides, when $d/r^s = 0.3$; $B_0 = 1$ T; $N = 10^{20}$ m^{-3}.

The working frequency range of models of n-GaAs waveguides with and without the external dielectric layer when the density of the electrons is constant $N = 10^{20}$ m^{-3} at different temperatures are presented in Table I.

TABLE I
WORKING FREQUENCY RANGES OF N-GAAS SEMICONDUCTOR AND SEMICONDUCTOR-DIELECTRIC WAVEGUIDES WHEN $N = 10^{20}$ M^{-3}

T, K		125	150	175	200
Δf, GHz	$d/r^s = 0$	23.0	24.1	24.1	24.4
	$d/r^s = 0.3$	19.9	22.0	28.4	19.6

It can be also noticed that the values of tensor of the relative dielectric permittivity significantly increase to thousands when the density of electrons in models of n-GaAs semiconductor and semiconductor-dielectric waveguides is increased till $N = 10^{21}$ m^{-3}. Such increase of the values of tensor of the relative dielectric permittivity causes distortions in phase characteristics of the waves. The obtained wave phase characteristics are presented in Figs 10 and 11. These characteristics are significantly shifted to the side of higher frequencies.

It is difficult to determine working frequency range Δfr^s of the models of semiconductor and semiconductor-dielectric waveguides with such phase characteristics. Phase shifters would not be able to work with such variation of characteristics, because the gyroelectric phase shifters must operate in a specific working frequency range.

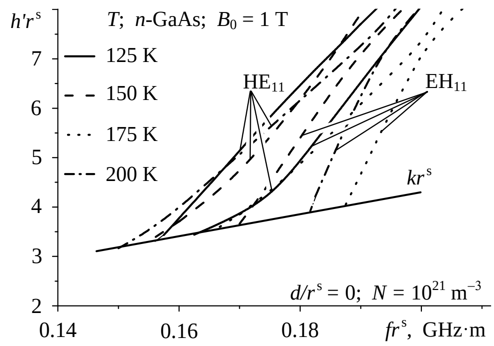

Fig. 10. Wave phase characteristics of models of gyroelectric n-GaAs semiconductor waveguides, when $d/r^s = 0$; $B_0 = 1$ T; $N = 10^{21}$ m^3.

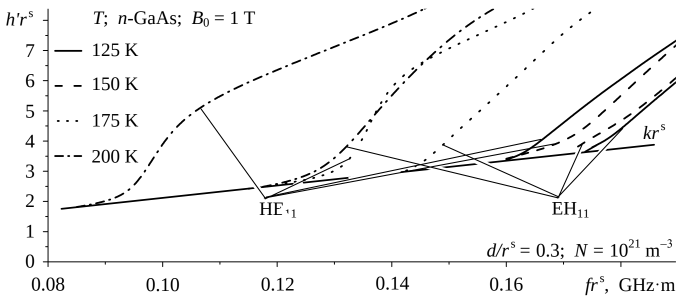

Fig. 11. Wave phase characteristics of models of gyroelectric n-GaAs semiconductor-dielectric waveguides, when $d/r^s = 0.3$; $B_0 = 1$ T; $N = 10^{21}$ m^{-3}.

It is possible to use models of n-GaAs semiconductor and semiconductor-dielectric waveguides in the manufacture of phase shifters when the density of electrons is equal to $5 \cdot 10^{18}$ m^{-3} and 10^{20} m^{-3}.

IV. Conclusions

The phase characteristics are practically unchanged in the models of *n*-GaAs semiconductor waveguides when the temperature varies from 125 K to 200 K and the density of electrons is equal to $N = (10^{17}–5\cdot10^{18})$ m^{-3}. Changes in wave phase coefficients are obtained in the models of waveguides with the external anisotropic dielectric layer.

The largest differences of wave phase coefficient on temperature are obtained in the models of *n*-GaAs gyroelectric waveguides when the density of electrons is increased till $N = 10^{21}$ m^{-3}.

Control using temperature is more effective in the models of *n*-GaAs semiconductor-dielectric waveguides in comparison with the models of *n*-GaAs semiconductor waveguides, because the external anisotropic dielectric layer consists of $Rb_{1-x}(ND_4)D_2PO_4$ ferroelectric, whose dielectric permittivity depends on temperature *T*. Therefore, this external anisotropic dielectric layer improves the control of thermal gyroelectric waveguides and models of phase shifters.

References

[1] C. Qin, B. Wang, H. Long, K. Wang and P. Lu, "Nonreciprocal Phase Shift and Mode Modulation in Dynamic Graphene Waveguides," in *Journal of Lightwave Technology*, vol. 34, no. 16, pp. 3877–3883, Aug. 2016. https://doi.org/10.1109/JLT.2016.2586959

[2] L. R. Chen, J. Wang, B. Naghdi and I. Glesk, "Subwavelength Grating Waveguide Devices for Telecommunications Applications," in *IEEE Journal of Selected Topics in Quantum Electronics*, vol. 25, no. 3, pp. 1–11, Nov. 2018. https://doi.org/10.1109/JSTQE.2018.2879015

[3] C. Yeh and F. Shimabukuro, *The Essence of Dielectric Waveguides*. Springer Science Business Media, New York, 2008.

[4] R. E. P. de Oliveira, and C. J. S. de Matos, "Analysis and Optimization of Graphene Based Waveguide Polarizers," in *Optical Fiber Communications Conference and Exhibition* (*OFC*), pp. 1–3, 2016.

[5] Y. Meng, S. Ye, Y. Shen, Q. Xiao, X. Fu, R. Lu, Y. Liu and M. Gong, "Waveguide Engineering of Graphene Optoelectronics—Modulators and Polarizers," in *IEEE Photonics Journal*, vol. 10, no. 1, pp. 1–18, Feb. 2018. https://doi.org/10.1109/JPHOT.2018.2789894

[6] Y. N. Gartstein and A. V. Malko, "Propagation and Absorption of Light in Planar Dielectric Waveguides With Two-Dimensional Semiconductors," in *Optics Express*, vol. 25, no. 19, pp. 23128–23136, 2017. https://doi.org/10.1364/OE.25.023128

[7] J. Xiao, Q. Q. Wei, D. G. Yang, P. Zhang, N. He, G. Q. Zhang and X. P. Chen, "Hybrid Plasmonics Slot THz Waveguide for Subwavelength Field Confinement and Crosstalk Between Two Waveguides," in *Journal of Selected Topics in Quantum Electronics*, vol. 23, no. 4, pp. 1–5, July-Aug. 2017. https://doi.org/10.1109/JSTQE.2017.2649939

[8] J. Cuadra, R. Verre, M. Wersäll, C. Krückel, V. Torres-Company, T. J. Antosiewicz and T. Shegai, "Hybrid Dielectric Waveguide Spectroscopy of Individual Plasmonic Nanoparticles," in *Aip Advances* vol. 7, no. 7, pp. 1–7, 2017. https://doi.org/10.1063/1.4986423

[9] E. Cojocaru, "Modes in Dielectric or Ferrite Gyrotropic Slab and Circular Waveguides, Longitudinally Magnetized, With Open and Completely or Partially Filled Wall," in *Journal of the Optical Society of America B*, vol. 27, no. 10, pp. 1965–1977, 2010. https://doi.org/10.1364/JOSAB.27.001965

[10] A. Budkin, M. Golubtsov, V. Litun and G. Slukin, "Generalized Design Technique for Fast Waveguide Ferrite Phase Shifters," in *Progress In Electromagnetics Research Symposium - Spring (PIERS)*, pp. 263–269, 2017. https://doi.org/10.1109/PIERS.2017.8261741

[11] R. Reese, M. Jost, H. Maune and R. Jakoby, "Design of a Continuously Tunable W-Band Phase Shifter in Dielectric Waveguide Topology," in *IEEE MTT-S International Microwave Symposium (IMS)*, pp. 180–183, 2017. https://doi.org/10.1109/MWSYM.2017.8058991

[12] V. V. Krutskikh, "The Element Base on the Basis of Semi-Shielded Dielectric Waveguides," in *24th International Crimean Conference Microwave & Telecommunication Technology*, pp. 1–2, 2014. https://doi.org/10.1109/CRMICO.2014.6959553

[13] B. R. Lavoie, P. M. Leung and B. C. Sanders, "Low-Loss Surface Modes and Lossy Hybrid Modes in Metamaterial Waveguides," *Photonics and Nanostructures-Fundamental and Applications*, vol. 10, no. 4, pp. 602–614, Oct. 2012. https://doi.org/10.1016/j.photonics.2012.05.010

[14] T. Amemiya, T. Kanazawa, S. Yamasaki and S. Arai, "Metamaterial Waveguide Devices for Integrated Optics," in *Materials* vol. 10, no. 9, pp. 1–17, 2017. https://doi.org/10.3390/ma10091037

[15] G. N. Jawad, C. I. Duff and R. Sloan, "A Millimeter-Wave Gyroelectric Waveguide Isolator," in *IEEE Transactions on Microwave Theory and Techniques*, vol. 65, no. 4, pp. 1249–1256, April 2017. https://doi.org/10.1109/TMTT.2016.2640298

[16] A. A. Shmat´ko, E. N. Odarenko, V. N. Mizemik and T. N. Rokhmanova, "Bragg Reflection and Transmission of Light by One-Dimensional Gyrotropic Magnetophotonic Crystal," in *2nd International Conference on Advanced Information and Communication Technologies (AICT)*, pp.123–125, 2017. https://doi.org/10.1109/AIACT.2017.8020108

[17] L. Nickelson, S. Asmontas, V. Malisauskas and V. Suguruvas, The Open Cylindrical Gyrotropic Waveguides, Technika, 2007.

[18] D. Plonis, A. Katkevičius, V. Mališauskas, A. Serackis and D. Matuzevičius, "Investigation of New Algorithms for Estimation of Losses in Microwave Devices Based on a Waveguide or a Meander Line," in *Acta Physica Polonica A*, vol. 129, no. 3, pp. 414–424, 2016. https://doi.org/10.12693/APhysPolA.129.414

[19] Y. J. Huang, W. T. Lu and S. Sridhar, "Nanowire Waveguide Made From Extremely Anisotropic Metamaterials," in *Physical Review A*, vol. 77, no. 6, pp. 1–11, 2008. https://doi.org/10.1103/PhysRevA.77.063836

[20] Q. Zhang, T. Jiang and Y. Feng, "Slow Wave Propagation in a Dielectric Cylindrical Waveguide With Anisotropic Metamaterial Cladding," in *Microwave Conference APMC 2009, Asia Pacific, 2009*, pp. 1242–1245. https://doi.org/10.1109/APMC.2009.5384439

[21] J. Banys, A. Kajokas, S. Lapinskas, A. Brilingas, J. Grigas, J. Petzelt and S. Kamba, "Microwave and Millimetre-Wave Dielectric Response of $Rb_{1-x}(ND_4)D_2PO_4$ Dipolar Glass," in *Journal of Physics-Condensed Matter*, vol. 14, no. 14, pp. 3725–3733, 2002. https://doi.org/10.1088/0953-8984/14/14/305

[22] Parameters of Semiconductors. [Online]. Available: http://www.ioffe.ru/SVA/NSM/Semicond/GaAs/index.html [Accessed: 3 October. 2018].

Darius Plonis received his B. sc., M. sc. and Ph.D. degrees in Electrical and Electronic Engineering from Vilnius Gediminas Technical University in 2008, 2010, and 2014, respectively. In 2017, he received the title of Associate Professor at VGTU.

He is an Associate Professor at the Department of Electronic Systems of Vilnius Gediminas Technical University. His main research interests include electromagnetic field theory, super-high frequency technologies and microwave devices, signal processing, multimedia and embedded systems.

Mr. Plonis is a member of the IEEE, an active member of IEEE Microwave Theory and Techniques, and currently serves as Secretary of IEEE Lithuania Section.

Address: Vilnius Gediminas Technical University, Faculty of Electronics, Naugarduko Str. 41 – 413, Vilnius, LT-03227, Lithuania.
E-mail: darius.plonis@vgtu.lt

Andrius Katkevičius obtained his B. sc., M. sc. and Ph.D. degrees in Electrical and Electronic Engineering from Vilnius Gediminas Technical University in 2007, 2009, and 2013, respectively. In 2017, he received the title of Associate Professor at VGTU.
He is an Associate Professor at the Department of Electronic Systems of Vilnius Gediminas Technical University. His main research interests include the electromagnetic field theory, super-high frequency technologies and microwave devices, signal processing, multimedia and embedded systems.
Address: Vilnius Gediminas Technical University, Faculty of Electronics, Naugarduko Str. 41 – 415, Vilnius, LT-03227, Lithuania.
E-mail: andrius.katkevicius@vgtu.lt

Diana Belova-Plonienė obtained her B. sc. and M. sc. degrees in Electronic Engineering from Vilnius Gediminas Technical University in 2009 and 2011, respectively.
Currently, she works as a Specialist at Vilnius Gediminas Technical University, Vilnius, Lithuania. Her research interests include computer vision, signal processing, communications and image analysis.
Address: Vilnius Gediminas Technical University, Faculty of Electronics, Naugarduko Str. 41 – 413, Vilnius, LT-03227, Lithuania.
E-mail: diana.belova-ploniene@vgtu.lt